Climate Dynamics (2025) 63:175
https://doi.org/10.1007/s00382-025-07660-5

ORIGINAL ARTICLE

Compound dry and hot extremes and their implications for fire activity over the Orinoco River Basin in northern South America

Paola A. Arias[1] · Alejandra Fernández-Berrío[1] · Valeria Bedoya-Pineda[1] · M. Yurani Acevedo-Ortiz[1] · J. Alejandro Martínez[2]

Received: 21 August 2024 / Accepted: 12 March 2025

Abstract

Compound dry and hot extremes (CDHE) have gained a pronounced relevance due to the observed increase in their frequency and the severity of their impacts on natural and human systems. The Orinoco River Basin, an ecoregion of great importance given its high biodiversity and the third largest river basin in South America, is vulnerable to these compound extremes because its extensive savannas are highly prone to fire activity. Here, we analyzed the occurrence of CDHE in this basin during the period 1981–2021. We compared different surface and atmospheric variables during drought periods (dry extremes) and CDHE (defined as periods with abnormally hot conditions during a meteorological drought event). Our results show that CDHE exhibit a larger precipitation deficit than dry extremes, exacerbating the meteorological drought. This stronger precipitation deficit is a response of weaker trade winds transporting moisture toward the region, in addition to stronger mid-tropospheric anticyclonic structures over the north Atlantic Ocean and the Caribbean Sea that advect dry air masses, inducing a deficit in total column water vapor and relative humidity at the mid-levels over the Orinoco. The moisture deficit during CDHE is also felt over the landmass, not only at surface but also deep soil layers, exacerbating the agricultural and ecological drought. Moreover, the decreased cloud cover associated with the enhanced precipitation deficit during CDHE increases the solar radiation reaching the surface, raising land temperature and reinforcing the drought impacts. Therefore, fire activity over the basin is enhanced during CDHE, increasing their associated burned area. This is very relevant since the savannas of the Orinoco are highly flammable and prone to fire, being burned with high frequency due to the practice of extensive livestock farming.

Keywords Hot extremes · Drought · Compound extremes · Fire activity · Orinoco · Northern South America

1 Introduction

The Sixth Assessment Report of the Intergovernmental Panel on Climate Change assesses that the occurrence of different extreme weather and climate events across the globe has become more frequent due to the increased emissions of greenhouse gases produced by human activities (IPCC 2021). In particular, human-induced climate change has caused an increase in the frequency and intensity of hot extremes, such as heat waves, on a planetary scale (IPCC 2021; Seneviratne et al. 2021). Also, the increases in global temperatures have intensified the hydrological cycle (Held and Soden 2006; Giorgi et al. 2011, 2014; Allan et al. 2020; Arias et al. 2021; Douville et al. 2021), evidenced by an increase in the frequency and intensity of extreme weather events, both dry and wet, in various continental regions (IPCC 2021; Seneviratne et al. 2021). Among the extreme events, droughts and hot extremes are of great importance due to their negative impacts in natural and human systems (Caretta et al. 2022; IPCC 2022; Parmesan et al. 2022). Furthermore, the simultaneous occurrence of these extremes can exacerbate the effects induced that each extreme when occurring in isolation (Arias et al. 2021; Ranasinghe et al. 2021; Seneviratne et al. 2021; Caretta et al. 2022).

✉ Paola A. Arias
paola.arias@udea.edu.co

[1] Grupo de Ingeniería y Gestión Ambiental (GIGA), Escuela Ambiental, Facultad de Ingeniería, Universidad de Antioquia, Medellín, Colombia

[2] Escuela Ambiental, Facultad de Ingeniería, Universidad de Antioquia, Medellín, Colombia

Published online: 28 March 2025

The increase in frequency and intensity of droughts and hot extremes, as well as their compound occurrence, leads to risks of food and water insecurity, and to negative impacts on biodiversity, human health and human migration (Zscheischler and Seneviratne 2017; Zscheischler et al. 2020; Caretta et al. 2022; Castellanos et al. 2022; Parmesan et al. 2022). For instance, the impacts of droughts are worse when they occur simultaneously with high temperatures, as hot conditions are among the drivers affecting the development of droughts due to the increase in evapotranspiration (Seneviratne 2012; Manning et al. 2019). Furthermore, the combination of high temperatures, drought and windy conditions (a.k.a. fire weather) can trigger the occurrence of fires, leading to impacts on agriculture, forestry, water supply systems, public health, and ecosystems (Ranasinghe et al. 2021). Therefore, the research of compound dry and hot extremes (CDHE) has gained a pronounced relevance during recent years.

The Orinoco River basin, located in northern South America, is a very important biodiverse region of the tropics (Romero et al. 2004; Bovolo et al. 2018). It has an area of 1’080,000 km^2, extending from the northern Colombian Amazon to the mouth of the Orinoco river’s delta in Venezuela (Gassón 2003). The Orinoco River runs through the Guiana´s Shield, the eastern slopes of the northern Andes, the Coastal Mountains, the plains of the Andes-Amazon transition region, and the flooded and non-flooded savannas over eastern Colombia and central-eastern Venezuela (Lasso et al. 2010). Despite its important biodiversity and being the third largest river basin in South America, studies focused on the hydroclimatology of the Orinoco River Basin are relatively scarce, in comparison to the two largest river basins of South America: the Amazon and the La Plata river basins.

The Orinoco River Basin is strongly influenced by the Caribbean Sea and the tropical north Atlantic (e.g. Poveda et al. 2006; Arias et al. 2020). It exhibits the lowest rainfall rates to the north, but further south, the region becomes rainier over the Guiana’s Shield and the transition toward the Amazon basin, with annual averages close to 3,800 mm. Two of the rainiest areas in this basin are the Andean foothills over the Meta-Cundinamarca departments and the Andean foothills of the Cauca River Basin in Colombia, with annual averages of 4,300 mm and 3,300 mm, respectively (Lasso et al. 2010). Valencia et al. (2024) find that savannas in the Llanos ecoregion (within the Orinoco River Basin) occur at mean annual precipitation (> 1500 mm) that would be associated with forest in other savanna regions (for example, the Cerrado in Brazil), suggesting a different behavior in this region. The Orinoco River Basin experiences its dry season between November and April, when the Intertropical Convergence Zone shows a southward migration and the trade winds intensify from the northeast over Venezuela. The wet season occurs between May and October, when trade wind speeds are weaker (Poveda et al. 2006; Arias et al. 2020). Hydroclimatology in this region is strongly influenced by El Niño-Southern Oscillation, exhibiting drier-than-normal conditions during El Niño and wetter-than-normal conditions during La Niña (Poveda et al. 2006; Álvarez and Poveda 2011).

In the Orinoco, fire activity is key in the ecological dynamics over meadows, grasslands, savannas and grasslands (Lavelle et al. 2014; Armenteras et al. 2021). Fire activity in this basin takes place mainly during the dry season, reaching a maximum in February. About 80% of the fires in this region are triggered by human activity (agricultural expansion, infrastructure, forest clearing, pest control and renewal of grasslands, accidentally, or deliberately) while 20% correspond to natural events (lightning strike or vegetation decomposition) (Lasso et al. 2010; Barreto and Armenteras 2020). Regardless of the causes behind fire triggering, the occurrence of fire-prone conditions, such as regional increases in temperature, aridity, drought, wind speed, and fuel abundance in forest and shrubland soils can lead to a greater frequency, intensity, extension, and severity of fires (Bolaño-Díaz et al. 2022; Castellanos et al. 2022). Even in ecosystems such as savannas, the occurrence of anomalous fire activity increases the exposure and vulnerability of the adjacent forest ecosystems adapted to fire, such as seasonally flooded forests (Bilbao et al. 2020; Flores and Holmgren 2021; Castellanos et al. 2022).

De Luca and Donat (2023) define CDHE as those days were maximum daily temperature exceeds the 90th percentile and monthly drought indices (Standardized Precipitation Index (SPI) and Standardized Precipitation and Evapotranspiration Index (SPEI) are below −1, identifying a recent increase of CDHE in northern South America, where the Orinoco River Basin is located. More recently, Feron et al. (2024) show that the Orinoco (they name it “the Maracaibo basin”) is the South American region that has warmed and dried the most since 1971, with increases up to 70 days per year in the annual amount of warm and dry days from 1971 to 2000 to 2001–2022. The extensive fires and animal mortality recorded during the 2014 drought in the department of Casanare in Colombia, in the western Orinoco (BBC 2014; El Espectador 2014), is evidence of the impacts of droughts in this region that are exacerbated when occurring in combination with extreme hot conditions. The susceptibility of the Orinoco River Basin to fire activity has been identified and discussed in the literature (e.g. Armenteras-Pascual et al. 2011; Hoyos et al. 2017; Bolaño-Díaz et al. 2022; Paredes-Trejo et al. 2023; García-Suabita et al. 2020).

This paper aims to identify CDHE over the Orinoco River Basin during the recent decades and characterize the main features of the regional atmospheric circulation behind these extremes and compare them with dry extremes. To do this, we used gridded, reanalysis and satellite data from different sources. Finally, this work intends to explore the behavior of fire activity during CDHE over this highly biodiverse but also highly vulnerable region of tropical South America.

2 Data and methodology

2.1 Study region

Our study region corresponds to the Orinoco River Basin, located in northern South America. We divided this basin into its northern (NORI) and southern (SORI) subdomains, given the contrast in the land cover between both regions (Fig. 1). NORI is characterized by the presence of Andean forests, high Andean forests, and paramo vegetation over the eastern Andes and their foothills, as well as by the tropical savannas in the central and western sub-basin. In contrast, SORI is covered by tropical humid forests, belonging to the transition zone towards the Amazon biome, shrubby vegetation associated with the Guiana's Shield, and wetlands (Romero et al. 2004). Some hydroclimate characteristics of NORI and SORI have been previously studied by Arias et al. (2020), who addressed the role of the Caribbean Sea and tropical north Atlantic sea surface temperatures (SSTs) on atmospheric moisture transport, precipitation, soil moisture, and vegetation activity in the Orinoco. Their findings indicate that precipitation and soil moisture in the Orinoco basin do not exhibit significant changes associated with SSTs, unlike atmospheric moisture recycling and transport, which increase with warmer SSTs in the tropical north Atlantic. This suggests that the link between SSTs and soil moisture in this region appears to be related not to changes in precipitation but to changes in atmospheric moisture recycling.

2.2 Gridded data

We used daily and monthly precipitation from the Climate Hazards Center InfraRed Precipitation with Stations (CHIRPS). CHIRPS is a quasi-global rainfall data set, available for the 50°S-50°N latitudinal domain, ranging from 1981 to the near-present. This dataset incorporates the Climate Hazards Center (CHP) climatology, 0.05° resolution satellite imagery, and in-situ station data to obtain a gridded rainfall product (Funk et al. 2015). The CHIRPS dataset can be downloaded from the site https://data.chc.ucsb.edu/products/CHIRPS-2.0/.

Daily maximum temperature (Tmax) from the Climate Hazards Center InfraRed Temperature with Stations (CHIRTS) was also considered. CHIRTS is a quasi-global (60°S–70°N) high-resolution (0.05° x 0.05°, approximately

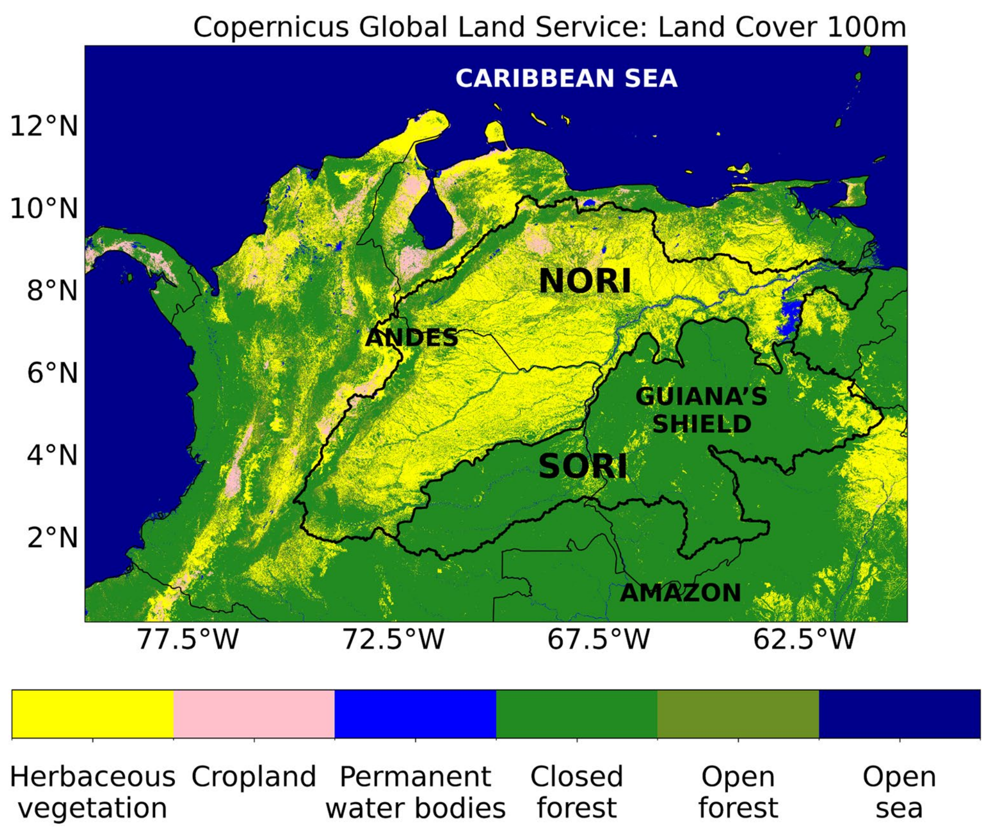

Fig. 1 Land cover over northern South America according to the Copernicus Global Land Service (CGLS; https://land.copernicus.eu/en). Thick black contours delimit the northern (NORI) and southern (SORI) Orinoco River Basin

5 km) dataset. This product directly combines estimates of Tmax based on satellites and stations to produce routinely updated data to support the monitoring of extreme temperatures and is available from the Climate Data Store (https://cds.climate.copernicus.eu/cdsapp#!/search?type=dataset) for the period 1983–2016.

2.3 Reanalysis data

To characterize atmospheric conditions during dry extremes and CDHE, we used daily fields of accumulated precipitation, Tmax, total column water vapor (TCWV), horizontal winds (zonal and meridional components) at 850 hPa and 500 hPa, 500 hPa relative humidity (RH), and 500 hPa geopotential height (Z500) from the ERA5 reanalysis (Hersbach et al. 2020) for the period 1981–2021. ERA5 is the most recent state-of-the-art reanalysis of the European Center for Medium-Range Weather Forecasts (ECMWF), with an equivalent 30 km horizontal grid size and 137 pressure levels. ERA5 data is accessible through the site https://www.ecmwf.int/en/forecasts/datasets/reanalysis-datasets/era5.

We also used daily soil moisture (SM) data from the ERA5-Land reanalysis for the period 1981–2021, with a spatial resolution of 0.1° x 0.1°. ERA5-Land is a reanalysis suite that provides a consistent view of the evolution of terrestrial variables with improved spatial resolution compared to ERA5 (Muñoz Sabater et al. 2021). We analyzed SM for surface (0–7 cm) and deep (7–289 cm) soil layers.

2.4 Satellite data

Considering that dry and hot weather conditions are some of the drivers of fire activity and/or propagation, we used active fires from the Terra and Aqua satellites of the Moderate Resolution Imaging Spectroradiometer (MODIS) for the period 2001–2021 at a horizontal resolution of 1 km, and available at https://firms.modaps.eosdis.nasa.gov/download/. This is a global product that locates fires from the fringe products (MOD14/MYD14; https://doi.org/10.5067/FIRMS/MODIS/MCD14ML.C6.1), identifying pixels that contain one or more active fires, as well as other thermal anomalies such as volcanoes. It is the most basic product for active fire detection and is recommended for long-term studies and time series analysis (Giglio et al. 2021).

We applied two filters to the MODIS data. We considered a first filter on the "Confidence" variable, selecting those fire pixels with a confidence in detection ≥ 95%. As a second filter, for the "Type" variable, we chose only the fire pixels inferred from vegetation (type 0). We selected the "fire pixels" with that percentage to use high quality data, reducing the number of false detections and facilitating the identification of real patterns in the spatial and temporal distribution of fires. Previous studies have used a confidence percentage greater than 80% for the same MODIS product (Hoyos et al. 2017; Barreto and Armenteras 2020; Yang et al. 2023).

We also used the combined MCD64A1 Version 6.1 Burned Area data product from Terra and Aqua (https://doi.org/10.5067/MODIS/MCD64A1.061). The approach of burned area mapping considers 500 m MODIS surface reflectance imagery, along with 1 km MODIS observations of active fires (Giglio et al. 2021). This version has significantly improved the detection of burned areas through calibration changes, including adjustments to the response focus with respect to the scanning angle, improving the accuracy of the reflectance bands of the Aqua and Terra MODIS sensors. Additionally, unwanted interference between Terra MODIS infrared channels has been corrected and a polarization correction has been applied to the reflective solar bands of L1B, improving the accuracy of reflected solar radiation measurements and, therefore, the detection of burned areas (Giglio et al. 2021). The MCD64A1 hybrid product detection algorithm uses a fire-sensitive Vegetation Index derived from atmospherically corrected surface reflectance bands from MODIS 5 and 7, to create dynamic thresholds applied to the composite data. The product data layers include detection date, uncertainty, quality control, and days of reliable change detection. The date is encoded in a single data layer as the ordinal day of the calendar year in which the fire occurred with values assigned to unburned land pixels and additional special values reserved for missing data and water grid cells (Giglio et al. 2021). The burned area information was downloaded using NASA's AρρEEARS analysis-ready sample extraction and exploration application (https://appeears.earthdatacloud.nasa.gov/).

2.5 Drought identification

To identify droughts in the Orinoco River Basin we analyzed three metrics: standardized precipitation anomalies (Psd), SPI and SPEI. These indices were computed from average monthly precipitation over both NORI and SORI for the 1981–2021 period.

The SPI, first developed by McKee et al. (1993), is based on a probabilistic precipitation approach, defined as the difference of mean precipitation over a specific time interval divided by the standard deviation. Once the time series is obtained at the desired frequency (monthly in our case), it is adjusted to the Gamma probability distribution function, in order to define the relationship between probability and precipitation. Once this relationship is established, the probability at any data point is calculated with an inverse normal estimate to estimate the precipitation deviation for a normally distributed probability function with zero mean and one standard deviation. The SPI has been used to estimate changes in meteorological droughts and to track precipitation deficit and surplus at multiple time scales (e.g., 1, 3, 9, or 12 months). This index allows differentiating between types of droughts (e.g. meteorological, agricultural and ecological, hydrological). However, the exclusion of evapotranspiration limits its usefulness, being an index that tracks moisture supply only from precipitation.

The SPEI was initially proposed by Vicente-Serrano et al. (2010) and is among the most widely used indices to identify and characterize droughts. This index uses not only precipitation (P) but also potential evapotranspiration (PET), in order to quantify the atmospheric evaporation demand and explicitly consider the effect of temperature throughout the drought. The SPEI is quantified using expression (1):

$$D_i = P_i - PET_i \quad (1)$$

where i is the time step (monthly in this case). Vicente-Serrano et al. (2010) found that the log-logistic (logarithmic) distribution correlates better with the D series, compared to other distribution parameters (Pearson III, lognormal). Thus, we used the log-logistic probability density function.

We classified as droughts those periods for which all the domain-average indices (SPI, SPEI and Psd) showed values below −1 standard deviation (SD) of their respective distribution simultaneously over both NORI and SORI. The SPI and Psd were estimated using CHIRPS (since these indices are precipitation-based). The SPEI was estimated using ERA5 (since it requires evapotranspiration). Drought intensity was assigned following the U.S. Drought Monitor methodology, based on SPEI thresholds: Abnormally Dry (-0.5 to -0.79), Moderate Drought (-0.8 to -1.29), Severe Drought (-1.3 to -1.59), Extreme Drought (-1.6 to -1.99), and Exceptional Drought (-2.0 or less) (https://droughtmonitor.unl.edu/About/AbouttheData/DroughtClassification.aspx). This selection allows the identification of drought period s that are consistent among databases and indices over both NORI and SORI, giving a more robust drought signal over the entire Orinoco basin.

2.6 Compound dry and hot extremes identification

In this work, hot extremes were considered as those days with daily Tmax anomalies exceeding the 90th percentile (P90) of the Tmax anomalies time series. We calculated the P90 from the Tmax anomalies distribution of the domain-average time series over each subdomain (NORI and SORI) during the 1981–2021 period. CDHE were defined as those events with at least 12 consecutive days within a drought (as identified from the monthly SPI and SPEI) with daily Tmax anomalies exceeding the P90. For comparison with CDHE, we defined dry extremes as those events with at least 8 consecutive days within a drought with daily Tmax anomalies below the P90.

The selection of two different duration threshold choices for CDHE (12 consecutive days) and dry extremes (8 consecutive days) relies on the fact that the CDHE in the Orinoco exhibit longer duration than the dry extremes. It means that the "recovery periods" of extreme temperatures during a drought have a shorter duration than the occurrence of combined hot and dry conditions during the drought. Since we are using precipitation anomalies and not cumulative precipitation during both types of events, we are not inducing biases in terms of larger cumulative precipitation deficits during the CDHE. The selection of a higher threshold for CDHE does not imply the selection of more intense droughts since the drought selection is based on monthly indices (such as SPI, SPEI, and Psd; see Sect. 2.5) therefore it does not consider the daily variations in precipitation.

According to ERA5, Tmax oscillates between approximately 27 °C during the wet season and 32 °C during the dry season in NORI, while it ranges from 26 °C in the wet season to 30 °C in the dry season in SORI. This indicates that there is not a significant difference in Tmax between the two seasons in both regions. Hence we did not consider seasonality in the estimation of hot extreme events because we aimed to determine when the Tmax anomalies could exceed the P90 threshold in each region, regardless of the season.

3 Recent droughts in the Orinoco River Basin

Figure 2 shows the monthly time series of Psd and SPI from CHIRPS and SPEI from ERA5 for NORI and SORI. In general, the three indices coincide in identifying the periods with surplus or deficit of precipitation over both regions. The indices show a similar variability over both subdomains of the Orinoco River Basin. Correlations between Psd and SPI are 0.943 in NORI and 0.971 in SORI. The Psd and SPI estimated from ERA5 (not shown) exhibit a similar behavior that those obtained from CHIRPS. Correlations between SPEI and the precipitation-based indices are much lower, with values around 0.2 for both regions. Despite this low correlation, estimated for the entire 1981–2021 period, the temporal variability of SPEI, SPI and Psd during droughts is much more similar, with values below −1SD for the three indices.

From Fig. 2, it is possible to identify drought periods of different categories that are common between NORI and SORI: 1982–1984, 1992–1993, 1995, 1997–1998, 2002–2003, 2009–2010, 2015–2016 and 2019–2020. These droughts range from Abnormally Dry to Extreme. No Exceptionally Extreme Droughts were identified over

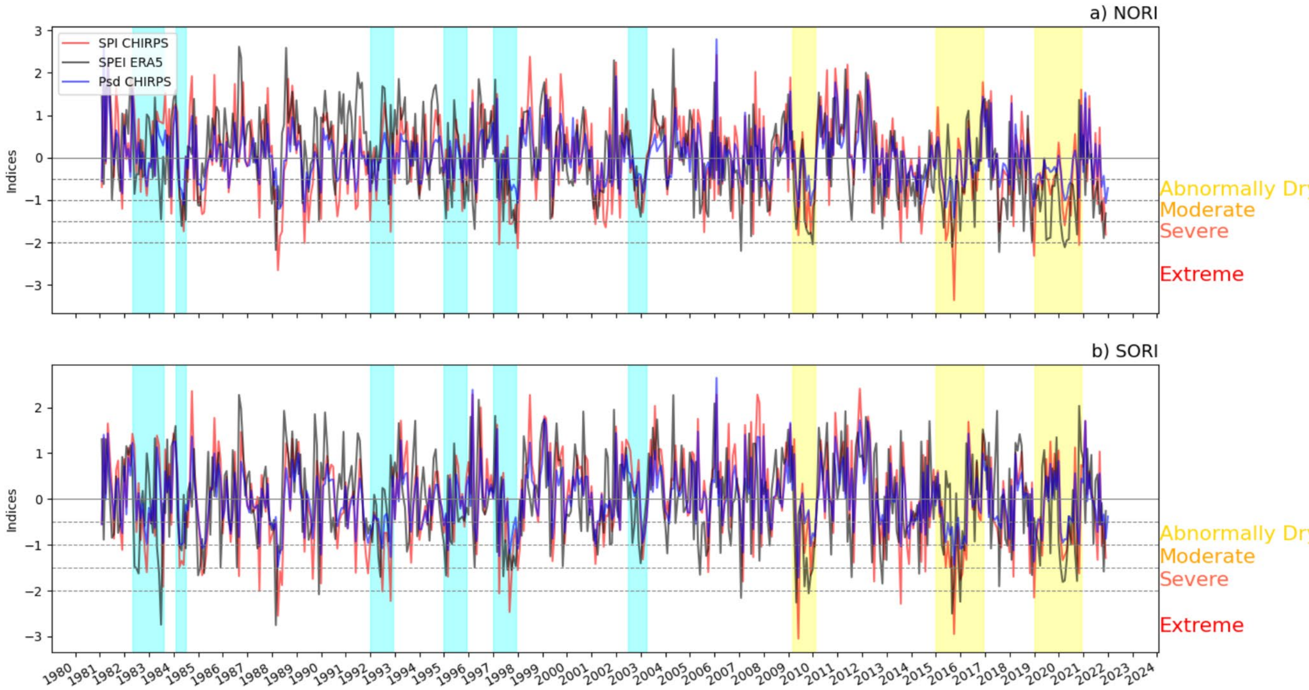

Fig. 2 Monthly time series of standardized precipitation anomalies (Psd) from CHIRPS (red line), Standardized Precipitation Index (SPI) from CHIRPS (blue line) and Standardized Precipitation and Evapotranspiration Index (SPEI) from ERA5 (black line) over the (**a**) northern (NORI) and (**b**) southern (SORI) Orinoco River Basin Data during the 1981–2021 period. Vertical shades indicate the drought events identified. The drought category, according to the U.S. Drought Monitor, is indicated: Abnormally Dry, Moderate, Severe, and Extreme. The blue shades show Abnormally Dry Droughts. The yellow shades correspond to Moderate, Severe, and Extreme Droughts

the Orinoco River Basin during the 1981–2021 period. Not surprisingly, many of these droughts occurred during a moderate or a very strong El Niño event: 1982–1983 (very strong), 1997–1998 (very strong), 2002–2003 (moderate), 2009–2010 (moderate), and 2015–2016 (very strong).

Unfortunately, the Orinoco basin is a region with a very low density in rain gauges. Figure S1 shows the distribution of meteorological stations in the Orinoco, according to the Hydrometeorological Service of Colombia (IDEAM). As observed, most of the rain gauge stations are located over the Andes piedmont and not over the lowlands of the Orinoco, where the droughts are detected. The low density of the rain gauge network in the Colombian Orinoco has been highlighted by previous studies (Mesa et al. 2021). The only rain gauge station located in the lowlands of the Colombian Orinoco is the Puerto Carreño station (star symbol in Figure S1a). As observed in Figure S1b, the IDEAM records in this station exhibit the drought signals suggested by the CHIRPS and ERA5 datasets, particularly during the events with the largest anomalies. This suggests that the drought signal depicted by CHIRPS and ERA5 is consistent with in situ data.

For further analysis, we focused on those droughts with SPI and SPEI values below −1 (Moderate, Severe, and Extreme Droughts) over both NORI and SORI: 02/2009-04/2010, 10/2013-06/2014, 04/2015-04/2016, 11/2018-08/2019, and 02/2020-08/2020. Figures S2 to S4 show a zoom for the 2008–2010, 2012–2016, and 2018–2021 periods for a clearer detail on the evolution of the indices throughout the drought events selected.

4 Compound dry and hot extremes in the Orinoco River Basin

4.1 Maximum temperature and precipitation anomalies

Figure 3 shows the domain-average daily Tmax anomalies over NORI and SORI from ERA5. It is clear that, although the Tmax anomalies exceed the P90 during different periods throughout the time series, this happens especially during the five drought events selected in the previous section. Following our definition for CDHE (periods of at least 12 consecutive days with daily Tmax anomalies exceeding the P90 during a drought event), we found that only the 02/2009-04/2010, 04/2015-04/2016, and 02/2020-08/2020 droughts exhibited the occurrence of CDHE. The 10/2013-06/2014 and 11/2018-08/2019 droughts do not show CDHE since the hot extremes (days with daily Tmax anomalies exceeding the P90) were more intermittent during these droughts and therefore the at-least-12-consecutive-days threshold

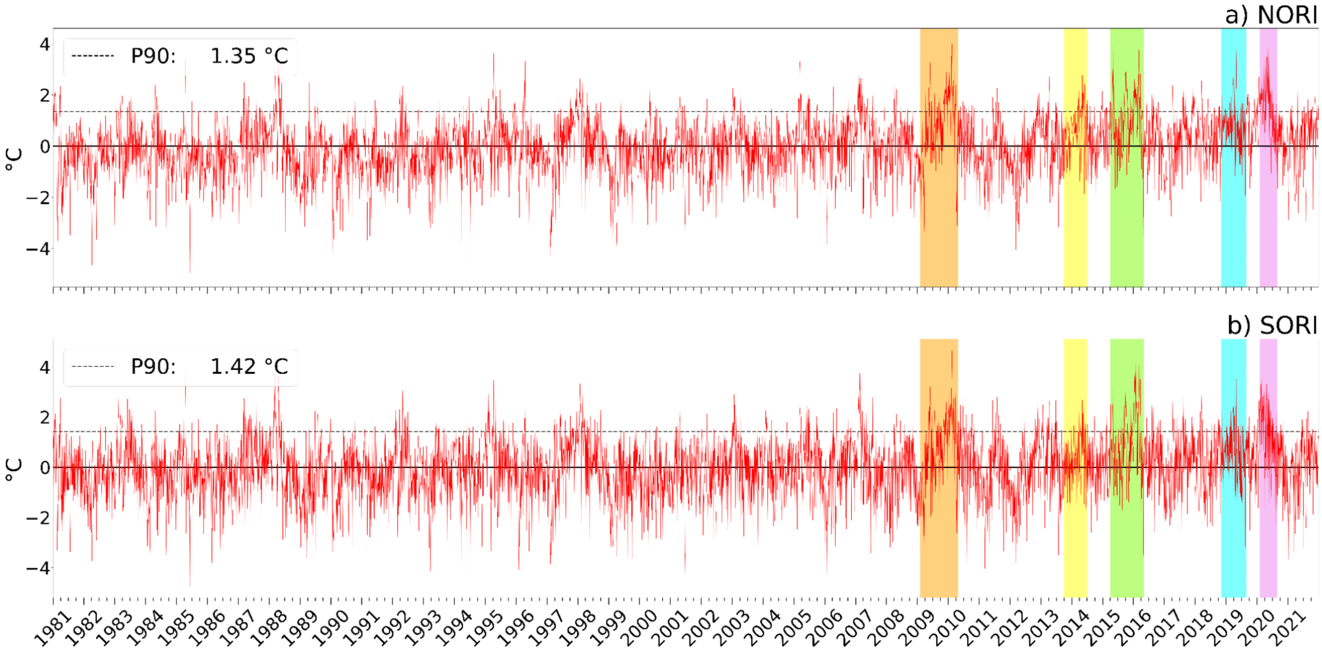

Fig. 3 Daily maximum temperature (Tmax) anomalies over the (**a**) northern (NORI) and (**b**) southern (SORI) Orinoco River Basin during the 1981–2021 period. The top dashed line indicates the 90th percentile (P90) of the anomalies time series. Shaded rectangles correspond to the five drought events identified from monthly data (orange: 02/2009-04/2010; yellow: 10/2013-06/2014; green: 04/2015-04/2016; cyan: 11/2018-08/2019; pink: 02/2020-08/2020). Data from ERA5

was not met (not shown). Tmax from CHIRTS (not shown) leads to similar conclusions. However, since CHIRTS data is only available for the 1983–2016 period, we considered the ERA5 Tmax to analyze the most recent CDHE in the Orinoco River Basin.

The daily Tmax anomalies time series over both NORI and SORI for the three drought events with CDHE occurrence are shown in Figure S5. The CDHE identified range between 12-days and 46-days duration. On the other hand, the dry extremes (periods of at least 8 consecutive days with daily Tmax anomalies below the P90 during the drought event) range between 8-days and 63-days duration. The 02/2009-04/2010 period exhibited three CDHE by the end of the drought while the initial stage was characterized by the occurrence of dry extremes (Figure S5a). By contrast, the 02/2020-08/2020 period had more CDHE (5 events) at the initial and mid stages of the drought (Figure S5c). The CDHE over the Orinoco River Basin are characterized by daily Tmax anomalies much larger than the P90 (1.35°C in NORI and 1.42°C in SORI), with anomalies reaching 4°C, particularly during the 02/2020-08/2020 drought (Figure S5c).

Figure 4 shows the frequency of exceedance of the daily Tmax P90 (a.k.a TX90 index) for NORI and SORI during the years for which a drought was detected (2009, 2010, 2013, 2014, 2015, 2016, 2018, 2019, 2020). In general, the exceedance of the daily Tmax P90 during the drought years is observed mainly during the dry season (January-March). As expected, the years with CDHE (2009, 2010, 2015, 2016, and 2020) have a higher frequency of exceedance of the daily TX90 index than drought years with no occurrence of CDHE. 2010 and 2016 have a higher TX90 index during the dry season. By contrast, 2020 has a higher TX90 index during February-May, exhibiting extreme hot conditions during the post-dry season (April-May). 2009 and 2015 exhibit a reduced TX90 in comparison to the other drought years, suggesting a less frequent occurrence of CDHE during these years. In contrast, these years have an exceedance of the daily TX90 index before the dry season, mainly for SORI.

The spatial composites of the daily Tmax anomalies during the CDHE and dry extremes are shown in Fig. 5. As suggested by Figs. 3 and 4, CDHE exhibit much larger Tmax anomalies than dry extremes, not only over the Orinoco River Basin but also in the surrounding areas. The daily Tmax positive anomalies are stronger over NORI. In this region, the Tmax anomalies reach values up to 3–4°C during the CDHE. Interestingly, the composite of dry extremes (Fig. 5b) shows slightly positive anomalies over some regions in NORI and SORI, which seems to be related with short duration precipitation events, as is described next.

Precipitation anomalies during CDHE indicate a strong deficit over northern South America, with an extension much larger than the Orinoco Basin, reaching regions in the northern Amazon and the northern Andes (Fig. 6a). Interestingly, dry extremes do not show a precipitation deficit (Fig. 6b). Here, it is important to recall how drought events and dry

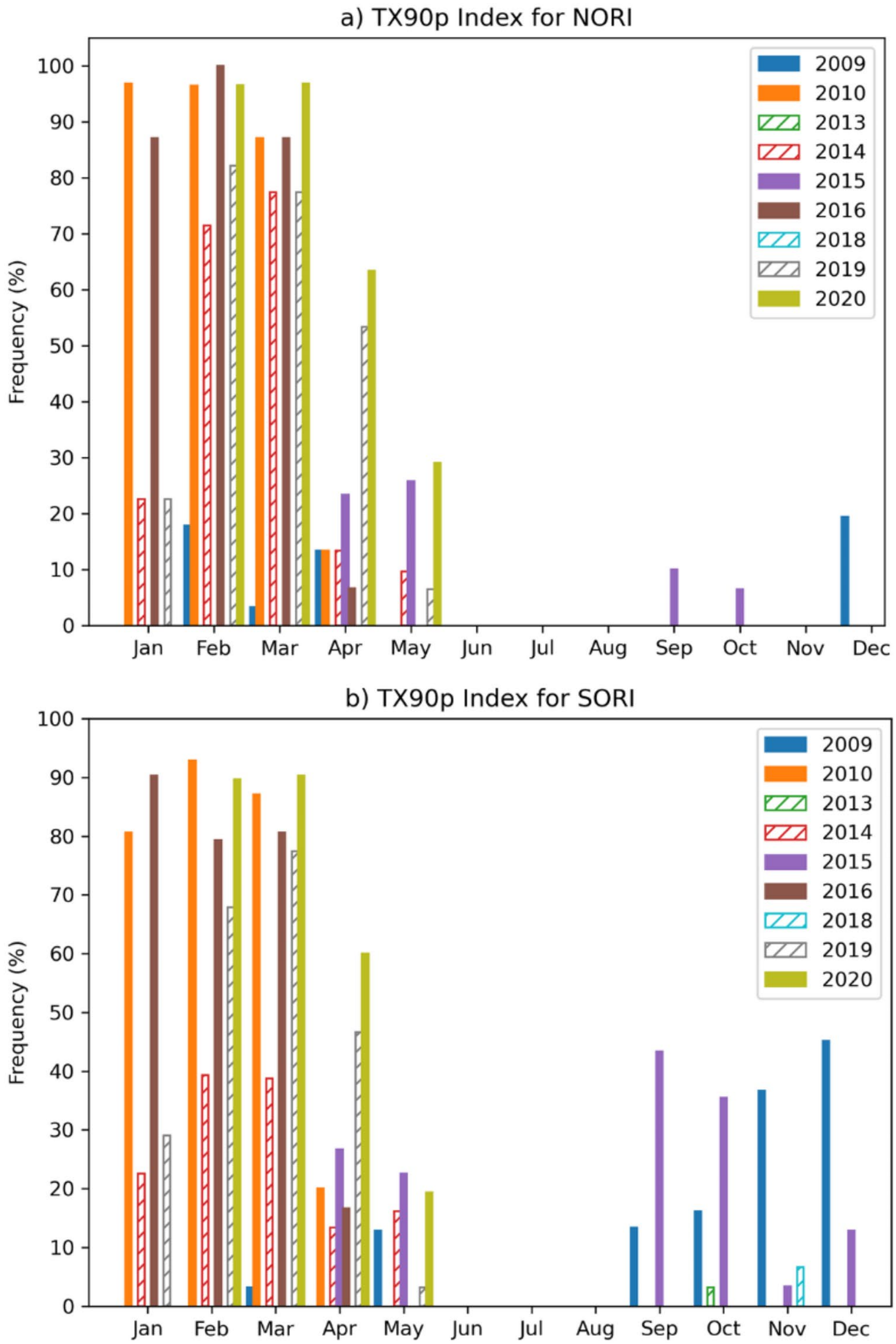

Fig. 4 Frequency of occurrence (%) of compound dry and hot extremes, according to the TX90p index (number of days in which the daily Tmax P90 is exceeded) during the years for which a drought was identified (Fig. 1), for the (**a**) northern (NORI) and (**b**) southern (SORI) Orinoco River Basin. Solid bars correspond to the drought years with the occurrence of compound dry and hot extremes (CDHE). Hatched bars correspond to the drought years for which there were no detection of CDHE. Data from ERA5

extremes were selected. Our identification of droughts is based on monthly Psd, SPI and SPEI. Therefore, we captured dry conditions at a monthly time scale. Dry extremes were selected considering periods of at least 8 consecutive days within a monthly-scale drought with daily Tmax anomalies below the P90. Therefore, although the monthly indices used to identify the droughts exhibit precipitation deficit during a particular month, the daily precipitation fields do not necessarily exhibit a deficit during all the days within the month, suggesting synoptic time scale variability in precipitation during the drought. These types of days may include relatively cool days (Tmax < P90), associated with days with precipitation.

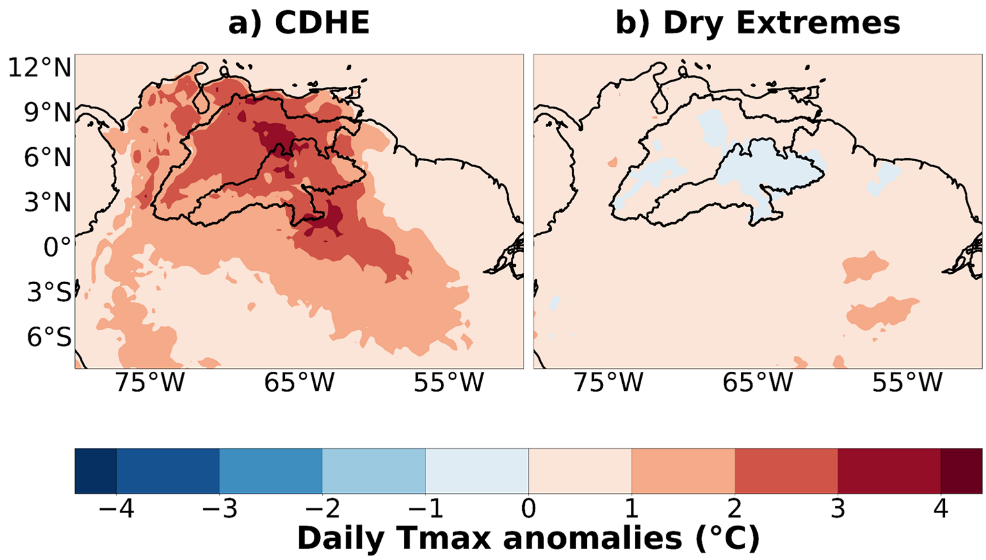

Fig. 5 Composites of daily maximum temperature (Tmax) anomalies during (**a**) compound dry and hot extremes (CDHE) and (**b**) dry extremes in the Orinoco River Basin. Thick contours delimit the northern and southern Orinoco River Basin. Data from ERA5

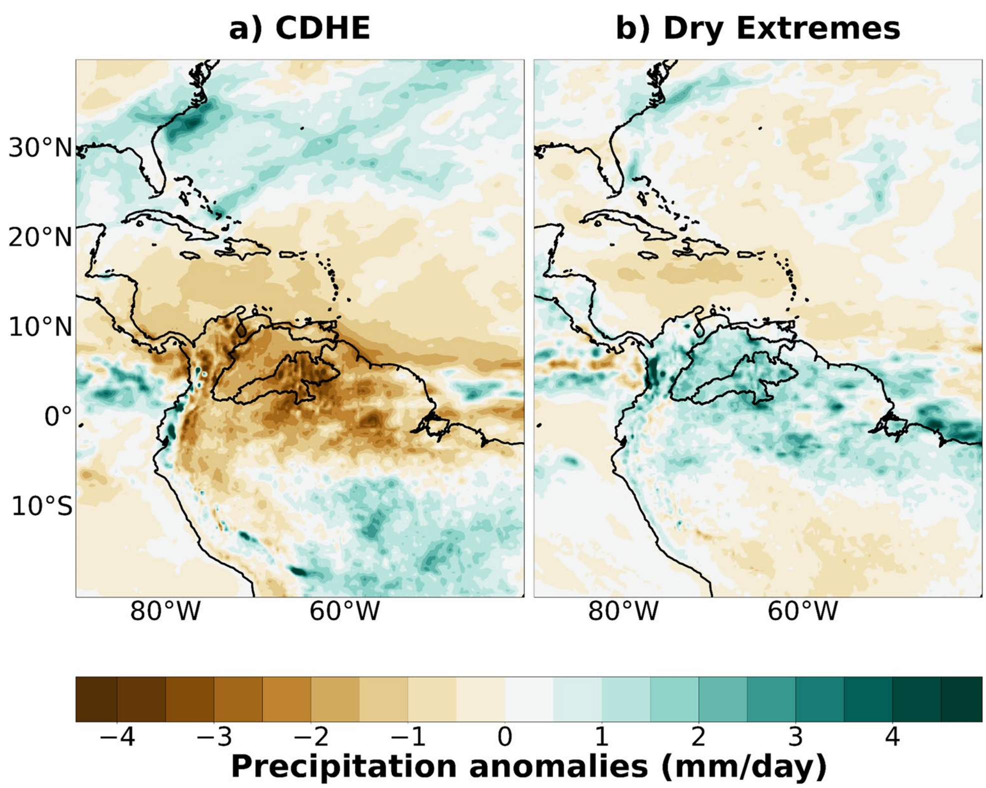

Fig. 6 Composites of precipitation anomalies during (**a**) compound dry and hot extremes (CDHE) and (**b**) dry extremes in the Orinoco River Basin. Thick contours delimit the northern and southern Orinoco River Basin. Data from CHIRPS

This is better observed in Figure S6, which presents the evolution of the spatial patterns of precipitation anomalies during the three droughts considered. Some periods of dry extremes exhibit precipitation deficits over the Orinoco, although they have smaller magnitudes with respect to the CDHE deficits. However, many of the periods with dry extremes show a clear recovery in precipitation, with anomalies larger than +3 mm/day, mainly during short periods (about 8–15 days-long) by the final stage of the drought. The domain average time series of daily Psd (Figure S5) shows that precipitation deficits are much stronger during CDHE in both sub-basins, exhibiting a recovery during the periods with no hot extremes (i.e. dry extremes). This suggests that although the monthly precipitation indices allow the identification of a drought, daily precipitation exhibits short recovery stages, highlighting the importance of considering precipitation variability within droughts at daily/weekly scales.

4.2 Atmospheric circulation

To better characterize the CDHE in the Orinoco River Basin, we analyzed the regional atmospheric circulation associated with these extremes and compared it with dry extremes. Figure 7 shows the composites of TCWV anomalies and 850 hPa winds during both types of extremes (Fig. 7a and b) as well as the corresponding 850 hPa wind anomalies (Fig. 7c and d). CDHE exhibit a clear deficit in TCWV over the Orinoco and Caribbean Sea (Fig. 7a), while

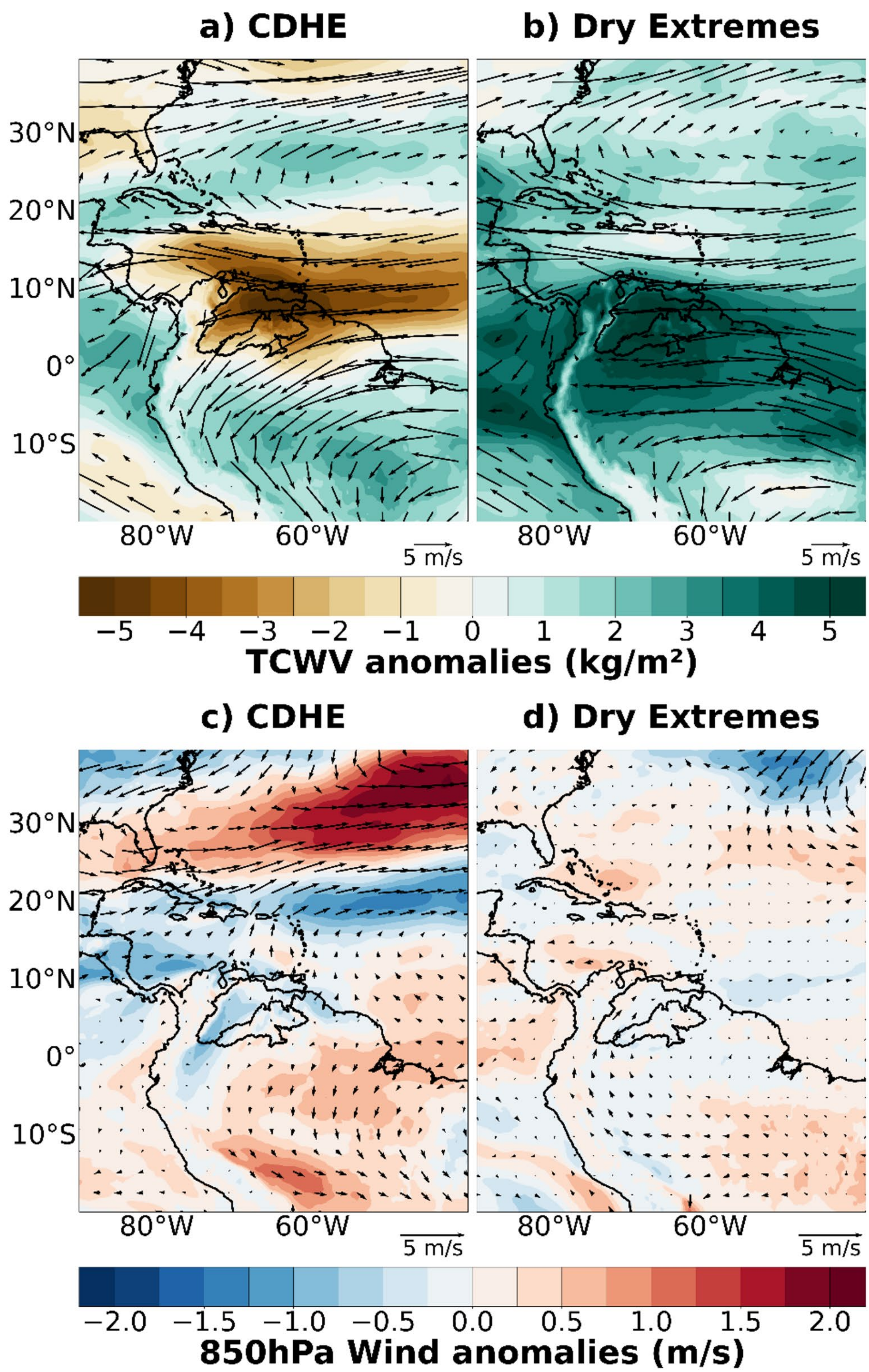

Fig. 7 Top: Composites of total column water vapor (TCWV) anomalies (shades) and 850 hPa horizontal winds (arrows) during (**a**) compound dry and hot extremes (CDHE) and (**b**) dry extremes in the Orinoco River Basin. Composites of 850 hPa horizontal wind anomalies during (**c**) CDHE and (**d**) dry extremes. Thick contours delimit the northern and southern Orinoco River Basin. Data from ERA5

dry extremes show a relative increase in total column water vapor (Fig. 7b). The low-level circulation shows a weakening of the trade winds over the Caribbean Sea and the tropical north Atlantic during the compound extremes. The 02/2009-04/2010 and 04/2015-04/2016 droughts occurred during moderate and very strong El Niño events, respectively, which are typically associated with a weakening of the Caribbean trade winds (e.g. Giannini et al. 2001). In particular, the northward component of the low-level wind anomalies over the Caribbean Sea surrounding the Orinoco (Fig. 7c) could produce a reduced water vapor import to the basin, contributing to the TCWV deficit.

To see if changes in regional circulation at the mid-troposphere reinforce this atmospheric moisture deficit during CDHE, Fig. 8 shows the composites of 500 hPa RH anomalies and 500 hPa winds (Fig. 8a and b) and the corresponding wind anomalies (Fig. 8c and d).

The CDHE exhibit reduced 500 hPa RH over the Orinoco River Basin, in association with an enhanced anticyclonic mid-tropospheric circulation over the tropical north Atlantic, the Caribbean Sea and the Orinoco River Basin. Stronger anticyclonic structures over the Caribbean Sea and the tropical north Atlantic bring dry air masses toward the Orinoco, product of the adiabatic descent of dry and warm masses within the mid-level high pressure system, advecting these dry masses toward northern South America through a divergent anticyclonic flow. The strengthening of the mid-level anticyclonic anomaly is further supported by the positive Z500 anomalies observed in the region during CDHE (Figure S7).

The moisture deficit over the Orinoco River basin during CDHE (Figs. 7 and 8) is felt not only in the atmosphere but also at the surface and deep soil layers (Fig. 9). For the dry extremes, the deficit in SM is detected mainly at the deep layers (Fig. 9d). In contrast, CDHE exhibit a much stronger deficit both in deep layers and in surface soil moisture (top layer) (Fig. 8a and c). Unlike the dry extremes, the SM deficit during CDHE is detected over large portions of northern South America, including the northern Amazon.

The analysis presented here suggests that the CDHE detected during the recent decades in the Orinoco River Basin have stronger precipitation deficits than the dry extremes (Fig. 6). A strengthened anticyclonic structure in the mid-levels of the troposphere over the Caribbean Sea and the north Atlantic Ocean during CDHE increases the advection of dry air masses toward the Orinoco River Basin (Fig. 8), inhibiting precipitation. This is strengthened by a weaker low-level atmospheric moisture transport by the trade winds (Fig. 7). In addition, the occurrence of extremely high temperatures during the CDHE (Fig. 5) enhances the atmospheric evaporation demand, exacerbating the SM deficit (Fig. 9) induced by the precipitation deficit.

5 Implications for fire activity

Among the impacts of CDHE is the enhancement of fire activity because these compound extremes provide favorable fire weather conditions. Figure 10a and b compare the total number of active fires in the Orinoco River Basin during CDHE and dry extremes, respectively. Clearly, NORI experiences more active fires during CDHE than during dry extremes (note that there are much more active fires in NORI: 8008 active fires during a total of 286 days under CDHE vs. 1716 active fires during a total of 383 days under dry extremes). Fire activity is much weaker over SORI, although it is also considerably increased during CDHE: 475 active fires during a total of 286 days under CDHE vs. 56 active fires during a total of 383 days under dry extremes. This remarkable difference in fire activity among both sub-basins is related to the characteristic savanna-like land cover in NORI (Fig. 1) that constitutes a pristine fuel for fire ignition, in addition to the land use practices over this region (Bedia et al. 2015; Armenteras et al. 2020; Chuvieco et al. 2012; Ynouye-Francés et al. 2021; Meza 2023; García-Suabita et al. 2020).

To see how the fire activity evolves within each drought, Figure S8 shows the location and number of active fires during each period of CDHE and dry extremes. The 04/2015-04/2016 and 02/2020-08/2020 droughts show that most of the fire activity occurs during CDHE, as suggested by Fig. 10a. However, not every CDHE event is characterized by an increase in fire activity. In fact, some periods with dry extremes show enhanced fire activity. This is the case for the 02/2009-04/2010 drought, which was characterized by increased fire activity during dry extremes at the initial stage (January-May/2009, corresponding to dry season months; Figure S8a). The next periods of dry extremes during this drought show a reduced fire activity, which increases again during the CDHE periods in November/2009-February/2010 (earlier dry season). Moreover, the CDHE exhibit much larger burned areas than the dry extremes, especially over the central NORI (Fig. 10c and d).

Figure 10a and S7 show that most of the active fires in the Orinoco occur during the dry season. This not only relates with the favorable fire weather conditions during this season but is highly linked to the land use practices, particularly associated with agriculture (Bedia et al. 2015; Armenteras et al. 2020; Chuvieco et al. 2012; Ynouye-Francés et al. 2021; Meza 2023). Regardless of the final causes of fire triggering, the consideration of the occurrence of more frequent fire weather conditions during CDHE should be very relevant in the management of fires over the Orinoco, given the considerably increased amount of active fires and large burned areas during these compound extremes (Fig. 10a and c). This highlights the importance of considering

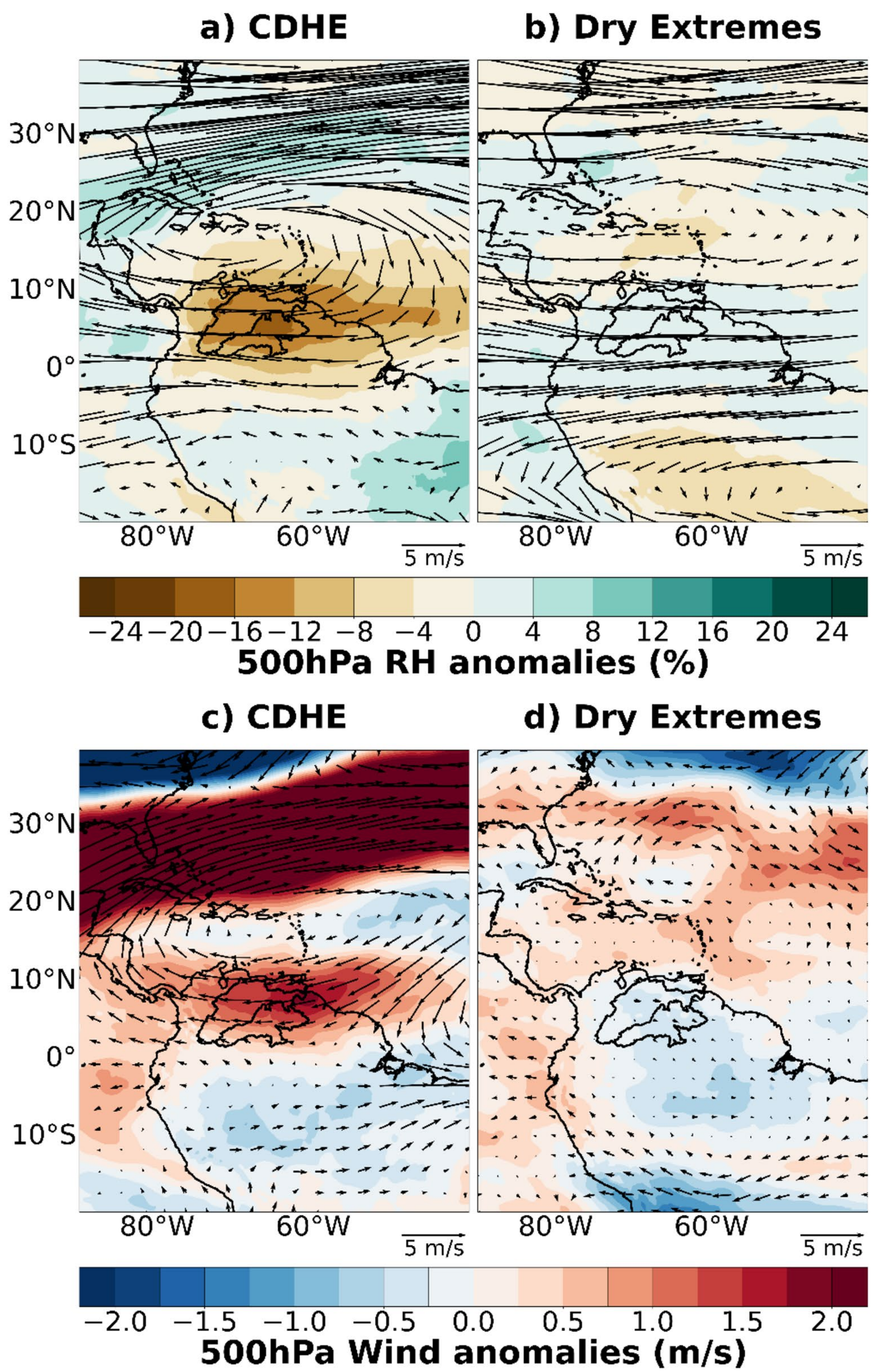

Fig. 8 Composites of 500 hPa relative humidity (RH) anomalies (shades) and 500 hPa horizontal winds (arrows) during (**a**) compound dry and hot extremes (CDHE) and (**b**) dry extremes in the Orinoco River Basin. Composites of 500 hPa horizontal wind anomalies during (**c**) CDHE and (**d**) dry extremes. Thick contours delimit the northern and southern Orinoco River Basin. Data from ERA5

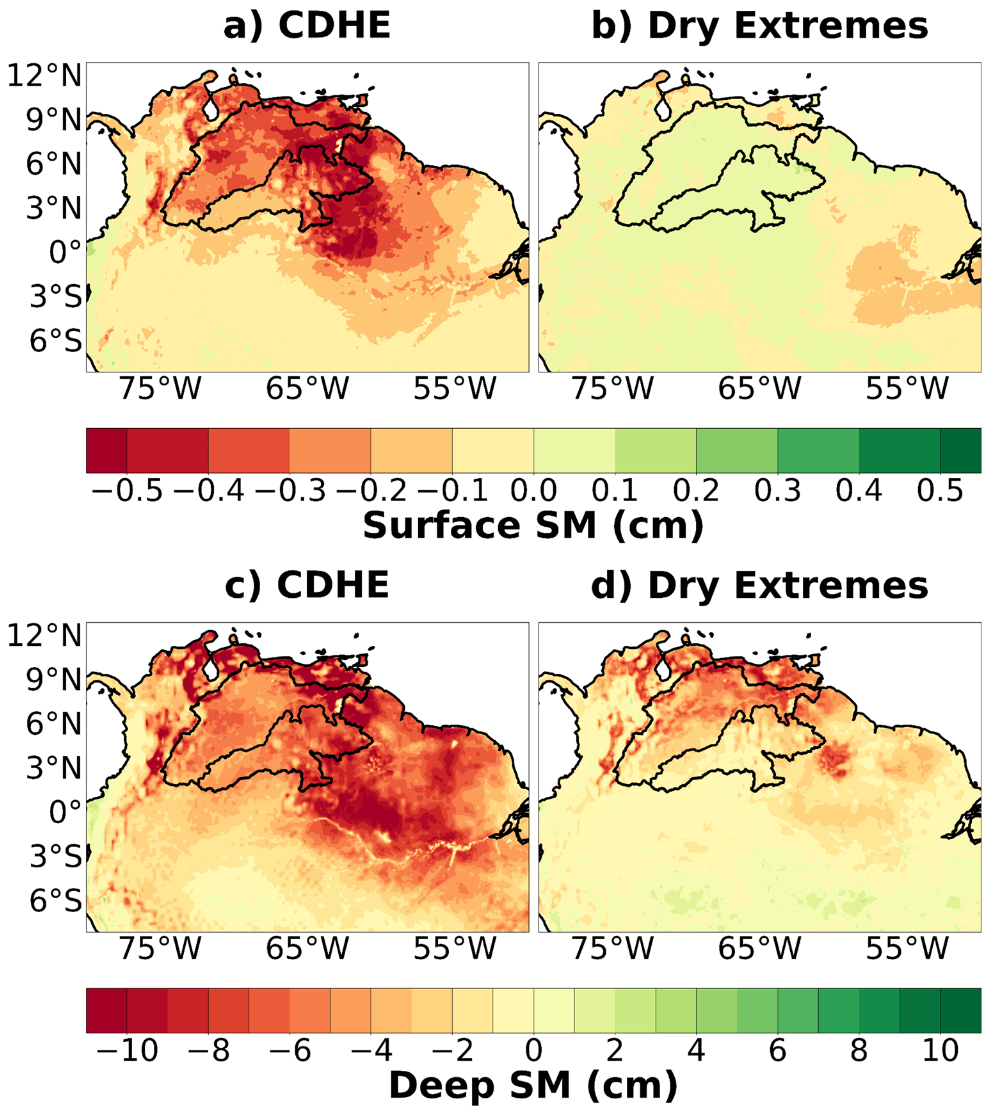

Fig. 9 Composites of soil moisture (SM) anomalies for the surface soil and the deep soil during (**a**–**c**) compound dry and hot extremes (CDHE) and (**b**–**d**) dry extremes in the Orinoco River Basin. Thick contours delimit the northern and southern Orinoco River Basin. Data from ERA5-Land

meteorological conditions, land cover and land use practices when assessing fire activity.

6 Summary and discussion

Through recent years, the Orinoco River Basin has been subject of attention in the understanding of compound dry and hot extremes (CDHE). The research of CDHE over this region becomes very relevant given the projected increases of frequency and intensity of agricultural and ecological droughts, hot extremes, and CDHE in the region as climate change scales (Hao et al. 2018; Arias et al. 2021; Ranasinghe et al. 2021; Seneviratne et al. 2021).

This work identified the most recent CDHE in the Orinoco River Basin. To do this, we selected drought events during the period 1981–2021 using monthly precipitation anomalies, the Standardized Precipitation Index and the Standardized Precipitation and Evapotranspiration Index. We focused on the droughts with indices below −1 (Moderate, Severe, and Extreme Droughts according to the U.S. Drought Monitor). Then, we selected hot extremes as those days with maximum temperature (Tmax) anomalies exceeding the 90th percentile of the daily Tmax time series (P90). CDHE events were defined as those periods with at least 12 consecutive days within a drought with daily Tmax exceeding the P90. Dry extremes were defined as those periods with at least 8 consecutive days within a drought with Tmax below the P90. With these definitions, we identified three drought events with the occurrence of CDHE: 02/2009-04/2010, 04/2015-04/2016, and 02/2020-08/2020. In particular, the 02/2009-04/2010 and 04/2015-04/2016 droughts occurred during moderate and very strong El Niño events, respectively.

To understand the difference between CDHE and dry extremes in the Orinoco River Basin, we analyzed Tmax,

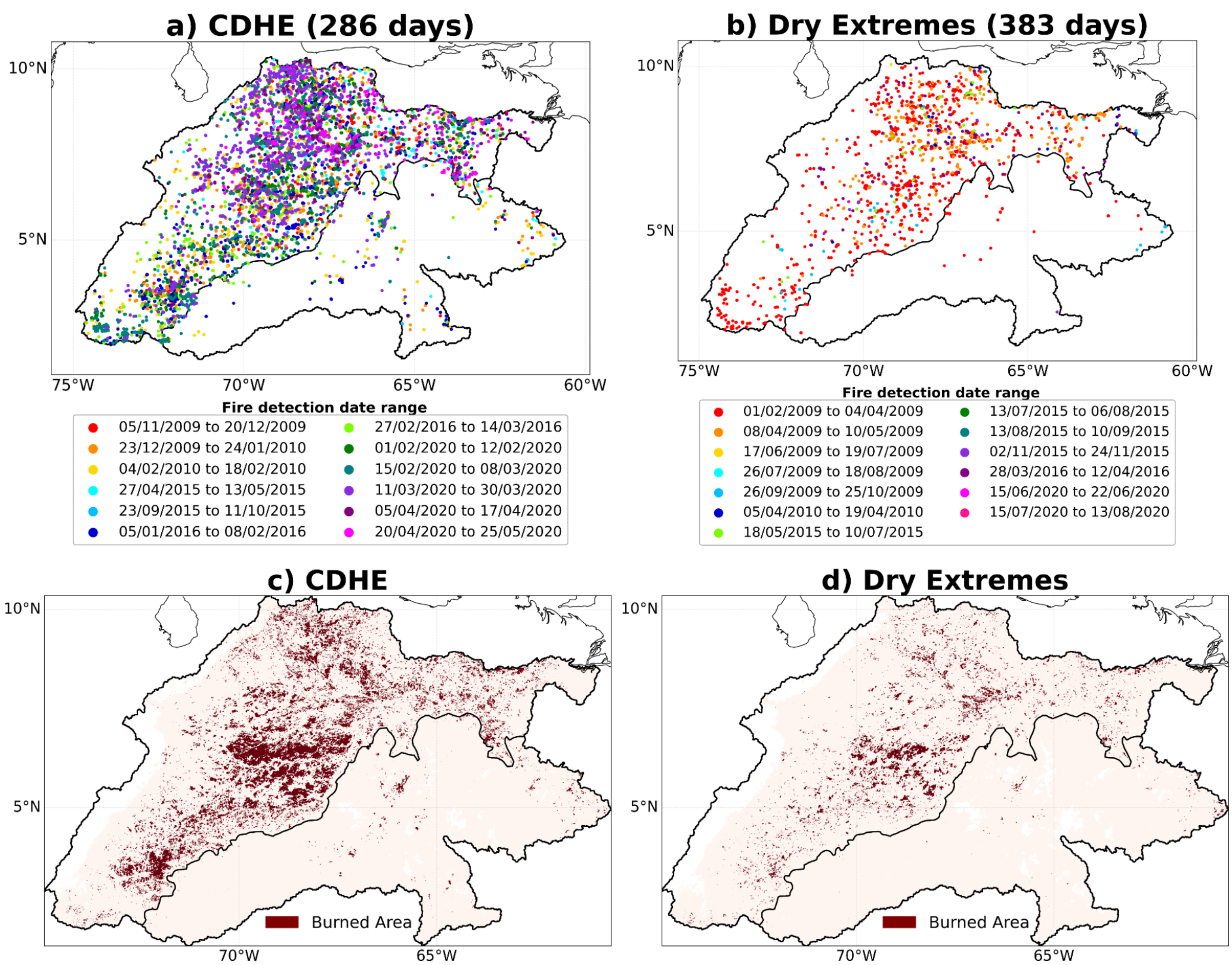

Fig. 10 Active fires during (**a**) compound dry and hot extremes (CDHE) and (**b**) dry extremes in the northern and southern Orinoco River Basin (delimited by the thick black contours). The number in brackets corresponds to the total number of days with the occurrence of each extreme. Colors indicate the date range (Day/Month/Year) corresponding to each fire detection. Burned area during (**c**) CDHE and (**d**) dry extremes. Data from MODIS

precipitation, soil moisture and the regional atmospheric circulation during both types of extremes. Our results show that CDHE have stronger precipitation deficits than the dry extremes (Fig. 6). This is caused by a strengthened anticyclonic structure in the mid-levels of the troposphere over the Caribbean Sea and the north Atlantic Ocean during CDHE, which increases the advection of hot and dry air masses toward the Orinoco River Basin (Fig. 8), inhibiting cloudiness and precipitation. Such inhibition is reinforced by a weaker low-level atmospheric moisture import to the basin by the trade winds (Fig. 7). Thus, the precipitation deficit induced by this anomalous circulation reinforces the meteorological drought. Also, the reduced cloud cover during CDHE contributes to increasing solar radiation reaching the surface, increasing sensible heat fluxes and temperatures over the Orinoco (Fig. 5). In turn, the occurrence of extremely high temperatures during the CDHE (Fig. 5) enhances the atmospheric evaporation demand, exacerbating the lack of soil moisture induced by the precipitation deficit (Fig. 9), thus reinforcing the agricultural and ecological drought.

A common consequence of anomalous CDHE is the strengthening of fire activity. Different studies in Latin America have shown the link between droughts and fires (e.g. Barni et al. 2021; Carvalho et al. 2021; Marengo et al. 2021; Oliveira-Júnior et al. 2022; Silvério et al. 2022; Oliveira et al. 2023). Meteorology is a crucial component in fire behavior, being the most dynamic and the most influenced by climate change (Collins 2014; Xu et al. 2020; Senande-Rivera et al. 2022). Variables such as temperature, relative humidity, and wind speed are key drivers of fire behavior and burn severity, as they control the rate of fire spread and the moisture content of the fuel (Fernández-Guisuraga et al. 2021). Therefore, we also analyzed the number of active fires and their respective burned area during CDHE and dry extreme events. The northern Orinoco is the region within the basin that is most affected by fires, which considerably increase in total number and burned area during the compound extremes (Fig. 10). Although the occurrence of CDHE provides favorable fire weather conditions, the land cover in the northern Orinoco (savanna-like vegetation; Fig. 1) is an important factor enhancing fire triggering and spreading because these savannas are highly flammable and prone to fire, being burned with high frequency due to the practice of extensive livestock farming (Armenteras et al. 2020; Meza 2023). The southern Orinoco, although much less affected by fires, also exhibited an increased occurrence of fire activity during the compound extremes (Fig. 10).

It is well known that fire has been used in the Orinoco, as in other regions of South America, for the management of grasslands and the renewal and expansion of areas intended for agricultural activities (Bedia et al. 2015; Armenteras et al. 2020; Chuvieco et al. 2012; Ynouye-Francés et al. 2021; Meza 2023). This practice is considered the most effective and economical for these purposes (Oliveira-Júnior et al. 2022). Different studies agree that the majority of ignition sources, approximately 90%, are due to deliberate human action, especially due to deforestation and the occurrence of long or extreme droughts (Chuvieco et al. 2012; Oliveira et al. 2022). Studies focused on other regions of South America reveal the direct link between human activities and fires (e.g. Barros-Rosa et al. 2022; Silveira et al. 2022). However, other authors point out that the factors that influence fire activity vary depending on the spatio-temporal scale. At a global level, meteorology is the main driver of fire activity, while, at a regional level, the drivers may be more diverse and, in some areas, related exclusively to land use activities (Senande-Rivera et al. 2022). Among the land uses related to fire activity in the Orinoco are extensive cattle, forest and savanna deforestation for wood extraction, mining, illegal crops, and intensive agriculture (e.g. Armenteras et al. 2005; Romero-Ruiz et al. 2010; Garcia-Suabita et al. 2020). Therefore we highlight the necessity of considering not only the meteorological but also the environmental conditions induced by land use for a comprehensive understanding of fire activity variability in this complex region. A deeper analysis of the relative contribution of meteorological and land use conditions needs to be assessed in further studies.

In this sense, although about 80% of the active fires in the Orinoco are triggered by human activities instead of by natural processes (Barreto and Armenteras 2020), the occurrence of prone fire weather conditions in this region contributes to worse the severity, intensity and extension of fires, as suggested by this work and observed in other regions in South America (de Magalhães and Evangelista 2022). This becomes increasingly important in the context of climate change since projections suggest more favorable fire weather over this region through the 21st century (e.g. Arias et al. 2021; Ranasinghe et al. 2021). Moreover, Valencia et al. (2024) show the importance of fire frequency and daily precipitation frequency during the dry season on the forest–savanna transition region between the Orinoco and the Amazon river basins (like the southern Orinoco region). Thus, these authors highlight that projections of future forest and savanna dynamics, and distribution should consider not only changes in mean annual precipitation but also changes in seasonal and intra-seasonal precipitation variability and fire-vegetation feedback. In this sense, our results highlight the occurrence of synoptic time scale precipitation variability within the droughts in the Orinoco River Basin, associated with the occurrence of hot extremes that exacerbate the meteorological drought during CDHE (Figures S5 and S6), enhancing fire activity over both the savannas of the northern Orinoco and the forest-savanna transition in the southern Orinoco (Fig. 10).

To our knowledge, there are still scarce studies that characterize the atmospheric circulation associated with CDHE in the Orinoco River Basin. This work contributes to a clearer understanding of the atmospheric mechanisms behind CDHE in the Orinoco River Basin that provide favorable conditions for fire activity. Specifically, the synoptic-scale mid-tropospheric anticyclonic activity over the tropical north Atlantic Ocean and Caribbean Sea is a strong feature behind CDHE (Fig. 8 and S6). Given the much better model performance in forecasting these synoptic features than precipitation, this finding could in turn contribute to the development of forecasting tools for these compound extremes in such a highly biodiverse but also vulnerable region.

Supplementary Information The online version contains supplementary material available at https://doi.org/10.1007/s00382-025-07660-5.

Acknowledgements This research was funded by Universidad de Antioquia through the grant TEM2022-55390 and by MINCIENCIAS through the program No. 80740-490-2020. This work was developed within the Andex Hydroclimatology Program (https://www.gewex.org/project/andex/), as a contribution of the Disciplinary Team on Ecological and Environmental Changes.

Author contributions P.A.A. and J.A.M. designed the research. P.A.A. wrote the funding proposals. A.F-B. and V.B-P. prepared the scripts and analyzed the data. M.Y.A-O. processed fire data. P.A.A. wrote the manuscript. All authors reviewed the manuscript and contributed to the analyses and discussion.

Funding Open Access funding provided by Colombia Consortium
This research was funded by Universidad de Antioquia through the grant TEM2022-55390 and by MINCIENCIAS through the program No. 80740-490-2020.

Data availability CHIRPS data can be accessed at https://data.chc.ucsb.edu/products/CHIRPS-2.0/. CHIRTS data can be downloaded from the site https://cds.climate.copernicus.eu/cdsapp#!/search?type=dataset. ERA5 data is available at the ECMWF portal: https://www.ecmwf.int/en/forecasts/datasets/reanalysis-datasets/era5.
ERA5-Land data is accessible at https://www.ecmwf.int/en/forecasts/datasets/reanalysis-datasets/era5. MODIS data is available at https://firms.modaps.eosdis.nasa.gov/download/.

Declarations

Competing interests The authors declare no conflicts of interest or competing interests.

References

Allan RP, BarloW M, Byrne MP et al (2020) Advances in Understanding large-scale responses of the water cycle to climate change. Ann NY Acad Sci 1472:49–75. https://doi.org/10.1111/nyas.14337

Álvarez DM, Poveda G (2011) Spatiotemporal dynamics of NDVI, soil moisture and ENSO in tropical South America. Remote Sens 14(2521). https://doi.org/10.3390/rs14112521

Arias PA, Martínez JA, Mejía JD, Pazos MJ, Espinoza JC, Wongchuig-Correa S (2020) Changes in normalized difference vegetation index in the orinoco and Amazon river basins: links to tropical Atlantic surface temperatures. J Clim 33(19):8537–8559. https://doi.org/10.1175/JCLI-D-19-0696.1

Arias PA, Bellouin N, Coppola E et al (2021) Technical summary. In: Zhai V, Pirani P A et al (eds) Climate change 2021: the physical science basis. Contribution of working group I to the sixth assessment report of the intergovernmental panel on climate change [Masson-Delmotte. Cambridge University Press, Cambridge, United Kingdom and New York, NY, USA, pp 33–144. https://doi.org/10.1017/9781009157896.002

Armenteras D, Romero M, Galindo G (2005) Vegetation fire in the savannas of the Llanos orientales of Colombia. World Resour Rev 17:531–543

Armenteras D, González TM, Vargas JO, Elizalde MCM, Oliveras I (2020) Incendios En ecosistemas Del Norte de Suramérica: Avances En La ecología Del Fuego tropical En Colombia, Ecuador y Perú. Caldasia 42:1–16. https://doi.org/10.15446/caldasia.v42n1.77353

Armenteras D, Meza MC, González TM, Oliveras I, Balch JK, Retana J (2021) Fire threatens the diversity and structure of tropical gallery forests. Ecosphere 12:e03347. https://doi.org/10.1002/ecs2.3347

Armenteras-Pascual D, Retana-Alumbreros J, Molowny-Horas R, Roman-Cuesta RM, Gonzalez-Alonso F, Morales-Rivas M (2011) Characterising fire Spatial pattern interactions with climate and vegetation in Colombia. Agric for Meteor 151(3):279–289. https://doi.org/10.1016/j.agrformet.2010.11.002

Barni PE, Rego ACM, Silva F, das CF et al (2021) Logging Amazon forest increased the severity and spread of fires during the 2015–2016 El Niño. Ecol Manag 500:119652. https://doi.org/10.1016/j.foreco.2021.119652

Barreto JS, Armenteras D (2020) Open data and machine learning to model the occurrence of fire in the ecoregion of Llanos Colombo–Venezolanos. Remote Sens 12:3921. https://doi.org/10.3390/rs12233921

Barros-Rosa L, Zanella de Arruda PH, Gomes Machado N, Pires-Oliveira JC, Eisenlohr PV (2022) Fire probability mapping and prediction from environmental data: what a comprehensive savanna-forest transition can tell Us. Ecol Manag 520:120354. https://doi.org/10.1016/j.foreco.2022.120354

BBC (2014) Casanare drought raises Colombia climate fears - BBC News. BBC Mundo. Accessed on 21 August 2024. https://bbc.in/3UcD6qu

Bedia J, Herrera S, Gutiérrez JM, Benali A et al (2015) Global patterns in the sensitivity of burned area to fire-weather: implications for climate change. Agric Meteorol 214–215:369–379. https://doi.org/10.1016/j.agrformet.2015.09.002

Bilbao B, Steil L, Urbieta IR et al (2020) Wildfires. In: Adaptation to Climate Change Risks in Ibero-American Countries — RIOCCADAPT Report [J. M. Moreno, C. Laguna-Defior, V. Barros, E. Calvo Buendía, J. A. Marengo, & U. Oswald Spring (Eds.)]. McGraw Hill, pp. 435–496. https://bit.ly/3TYsWJR

Bolaño-Díaz S, Camargo-Caicedo Y, Soro TD, N'Dri AB, Bolaño-Ortiz TR (2022) Spatio-Temporal characterization of fire using MODIS data (2000–2020) in Colombia. Fire 5(5):134. https://doi.org/10.3390/fire5050134

Bovolo CI, Wagner T, Parkin G et al (2018) The Guiana shield rainforests—Overlooked guardians of South American climate. Environ Res Lett 13(7):074029. https://doi.org/10.1088/1748-9326/aacf60

Caretta MA, Mukherji A, Arfanuzzaman M et al (2022) Water. In: Roberts DC, Tignor M et al (eds) Climate change 2022: impacts, adaptation and vulnerability. Contribution of working group II to the sixth assessment report of the intergovernmental panel on climate change [Pörtner H-O. Cambridge University Press, Cambridge, UK and New York, NY, USA, pp 551–712. https://doi.org/10.1017/9781009325844.006

Carvalho NS, Anderson LO, Nunes CA et al (2021) Spatio-temporal variation in dry season determines the Amazonian fire calendar. Environ Res Lett 16:125009. https://doi.org/10.1088/1748-9326/ac3aa3

Castellanos EJ, Lemos MF, Astigarraga L et al (2022) Central and South America. In: Roberts H-O, Tignor DC M et al (eds) Climate change 2022: impacts, adaptation and vulnerability. Contribution of working group II to the sixth assessment report of the intergovernmental panel on climate change [Pörtner. Cambridge University Press, Cambridge, UK and New York, NY, USA, pp 1689–1816. https://doi.org/10.1017/9781009325844.014

Chuvieco E, Cifuentes Y, Hantson S et al (2012) Comparación Entre Focos de Calor MODIS y perímetros de área Quemada En incendios mediterráneos. Rev Teledetec Rev Asoc Esp Teledetec 37:9–22

Collins BM (2014) Fire weather and large fire potential in the Northern Sierra Nevada. Agric Meteorol 189–190:30–35. https://doi.org/10.1016/j.agrformet.2014.01.005

De Luca P, Donat MG (2023) Projected changes in hot, dry, and compound hot-dry extremes over global land regions. Geophys Res Lett 50. https://doi.org/10.1029/2022GL102493.:e2022GL102493 de Magalhães N, Evangelista H (2022) Human activity behind the unprecedented 2020 wildfire in Brazilian wetlands (Pantanal). Front Environ Sci 14:1–15. https://doi.org/10.3389/fenvs.2022.888578

Douville H, Raghavan K, Renwick J et al (2021) Water cycle changes. In: Zhai V, Pirani P A et al (eds) Climate change 2021: the physical science basis. Contribution of working group I to the sixth assessment report of the intergovernmental panel on climate change [Masson-Delmotte. Cambridge University Press, Cambridge, United Kingdom and New York, NY, USA, pp 1055–1210. https://doi.org/10.1017/9781009157896.010

El Espectador (2014) Sequía En Casanare consumió En total 45.395 hectáreas. Accessed on 21 August 2024. https://bit.ly/43V1hxS

Fernández-Guisuraga JM, Suárez-Seoane S, García-Llamas P, Calvo L (2021) Vegetation structure parameters determine high burn severity likelihood in different ecosystem types: A case study in a burned mediterranean landscape. J Environ Manage 288:112462. https://doi.org/10.1016/j.jenvman.2021.112462

Feron S, Cordero RR, Damiani A et al (2024) South America is becoming warmer, drier, and more flammable. Commun Earth Environ 5:501. https://doi.org/10.1038/s43247-024-01654-7

Flores BM, Holmgren M (2021) White-Sand savannas expand at the core of the Amazon after forest wildfires. Ecosystems 24(7):1624–1637. https://doi.org/10.1007/s10021-021-00607-x

Funk C, Peterson P, Landsfeld M et al (2015) The climate hazards infrared precipitation with stations—a new environmental record for monitoring extremes. Sci Data 2:150066. https://doi.org/10.1038/sdata.2015.66

Garcia-Suabita W, Pacheco MJ, Armenteras D (2020) Multitemporal dynamics of fuels in forest systems present in the Colombian orinoco river basin forests. Fire 7(6):171. https://doi.org/10.3390/fire7060171

Gassón RA (2003) Orinoquia: the archaeology of the orinoco river basin. J World Prehist 16:237–311. https://doi.org/10.1023/A:1020978518142

Giannini A, Chiang JCH, Cane MA et al (2001) The ENSO teleconnection to the tropical Atlantic Ocean: contributions of the remote and local SSTs to rainfall variability in the tropical Americas. J Clim 14:4530–4544. https://doi.org/10.1175/1520-0442(2001)014%3C4530:TETTTT%3E2.0.CO;2

Giglio L, Justice C, Boschetti L, Roy D (2021) MODIS/Terra + Aqua burned area monthly L3 global 500m SIN grid V061. https://doi.org/10.5067/MODIS/MCD64A1.061

Giorgi F, Im E, Coppola E, Diffenbaugh NS, Gao XJ, Mariotti L, Shi Y (2011) Higher hydroclimatic intensity with global warming. J Clim 24:5309–5324. https://doi.org/10.1175/2011JCLI3979.1

Giorgi F, Coppola E, Raffaele F (2014) A consistent picture of the hydroclimatic response to global warming from multiple indices: models and observations. J Geophys Res Atmos 119:695–708. https://doi.org/10.1002/2014JD022238

Hao Z, Hao F, Singh VP, Zhang X (2018) Changes in the severity of compound drought and hot extremes over global land areas. Environ Res Lett 13(12):124022. https://doi.org/10.1088/1748-9326/aaee96

Held IM, Soden BJ (2006) Robust responses of the hydrological cycle to global warming. J Clim 19:5686–5699. https://doi.org/10.1175/JCLI3990.1

Hersbach H, Bell B, Berrisford P et al (2020) The ERA5 global reanalysis. Q J R Meteorol Soc 146:1999–2049. https://doi.org/10.1002/qj.3803

Hoyos N, Correa-Metrio A, Sisa A et al (2017) The environmental envelope of fires in the Colombian Caribbean. Appl Geogr 84:42–54. https://doi.org/10.1016/j.apgeog.2017.05.001

IPCC (2021) Summary for policymakers. Climate change 2021 – The physical science basis. Cambridge University Press, Cambridge, UK and New York, NY, USA, pp 3–32. https://doi.org/10.1017/9781009157896.001

IPCC (2022) Summary for policymakers. Climate change 2022 – Impacts, adaptation and vulnerability. Cambridge University Press, Cambridge, UK and New York, NY, USA, pp 3–33. https://doi.org/10.1017/9781009325844.001

Lasso CA, Usma Oviedo J, Trujillo Gonzalez F, Rial A (2010) Biodiversidad de La Cuenca Del Orinoco: bases científicas Para La identificación de áreas prioritarias Para La conservación y Uso sostenible de La Biodiversidad. Instituto de investigación de Recursos Biológicos Alexander von Humboldt

Lavelle P, Rodriguez N, Arguello O et al (2014) Soil ecosystem services and land use in the rapidly changing orinoco river basin of Colombia. Agric Ecosys Environ 185:106–117. https://doi.org/10.1016/j.agee.2013.12.020

Manning C, Widmann M, Bevacqua E, Van Loon AF, Maraun D, Vrac M (2019) Increased probability of compound long-duration dry and hot events in Europe during summer (1950–2013). Environ Res Lett 14(9). https://doi.org/10.1088/1748-9326/ab23bf

Marengo JA, Cunha AP, Cuartas LA et al (2021) Extreme drought in the Brazilian Pantanal in 2019–2020: characterization, causes, and impacts. Front Water 3:1–20. https://doi.org/10.3389/frwa.2021.639204

McKee TB, Doesken NJ, Kleist J (1993) The relationship of drought frequency and duration to time scales. Eighth Conference on Applied Climatology, 17–22 January 1993, Anaheim, California

Mesa O, Urrea V, Ochoa A (2021) Trends of hydroclimatic intensity in Colombia. Climate 9(7):120. https://doi.org/10.3390/cli9070120

Meza MC (2023) Efectos de los incendios forestales sobre la resiliencia de bosques tropicales de tierras bajas (Tesis de Doctorado). Universidad Nacional de Colombia, Bogot&#225

Muñoz-Sabater J, Dutra E, Agustí-Panareda A et al (2021) ERA5-Land: a state-of-the-art global reanalysis dataset for land applications. Earth Syst Sci Data 13:4349–4383. https://doi.org/10.5194/essd-13-4349-2021

Oliveira U, Soares-Filho B, Bustamante M, Gomes L, Ometto JP, Rajão R (2022) Determinants of fire impact in the Brazilian biomes. Front Glob Change 5:735017. https://doi.org/10.3389/ffgc.2022.735017

Oliveira JG de, Massi KG, Bortolozo LAP, Cunha APM do A (2023) The influence of climate parameters on fires in the Paraíba do Sul river Valley, Southeast Brazil. Rev Ambiente Água 18:e2923. https://doi.org/10.4136/ambi-agua.2923

Oliveira-Júnior JF, Shah M, Abbas A et al (2022) Spatiotemporal analysis of fire foci and environmental degradation in the biomes of Northeastern Brazil. Sustainability 14:6935. https://doi.org/10.3390/su14116935

Paredes-Trejo F, Olivares BO, Movil-Fuentes Y, Arevalo-Groening J, Gil A (2023) Assessing the Spatiotemporal patterns and impacts of droughts in the orinoco river basin using Earth observations data and surface observations. Hydrology 10:195. https://doi.org/10.3390/hydrology10100195

Parmesan C, Morecroft MD, Trisurat Y et al (2022) Terrestrial and freshwater ecosystems and their services. In: Roberts H-O, Tignor DC M et al (eds) Climate change 2022: impacts, adaptation and vulnerability. Contribution of working group II to the sixth assessment report of the intergovernmental panel on climate change [Pörtner. Cambridge University Press, Cambridge, UK and New York, NY, USA, pp 197–377. https://doi.org/10.1017/9781009325844.004

Poveda G, Waylen PR, Pulwarty RS (2006) Annual and inter-annual variability of the present climate in Northern South America and Southern Mesoamerica. Palaeogeogr Palaeoclimatol Palaeoecol 234(1):3–27. https://doi.org/10.1016/j.palaeo.2005.10.031

Ranasinghe R, Ruane AC, Vautard R et al (2021) Climate change information for regional impact and for risk assessment. In: Zhai

V, Pirani P A et al (eds) Climate change 2021: the physical science basis. Contribution of working group I to the sixth assessment report of the intergovernmental panel on climate change [Masson-Delmotte. Cambridge University Press, Cambridge, United Kingdom and New York, NY, USA, pp 1767–1926. https://doi.org/10.1017/9781009157896.014

Romero M, Galinod OJ, Armenteras D (2004) La Cuenca Del orinoco En El contexto mundial. Instituto de Investigación de Recursos Biológicos Alexander van Humboldt

Romero-Ruiz M, Etter A, Sarmiento A, Tansey K (2010) Spatial and Temporal variability of fires in relation to ecosystems, land tenure and rainfall in savannas of Northern South America: Spatial and Temporal variability of fires. Glob Change Biol 16:2013–2023. https://doi.org/10.1111/j.1365-2486.2009.02081.x

Senande-Rivera M, Insua-Costa D, Miguez-Macho G (2022) Spatial and Temporal expansion of global wildland fire activity in response to climate change. Nat Commun 13:1208. https://doi.org/10.1038/s41467-022-28835-2

Seneviratne S (2012) Historical drought trends revisited. Nature 491:338–339. https://doi.org/10.1038/491338a

Seneviratne SI, Zhang X, Adnan M et al (2021) Weather and climate extreme events in a changing climate. In: Zhai V, Pirani P A et al (eds) Climate change 2021: the physical science basis. Contribution of working group I to the sixth assessment report of the intergovernmental panel on climate change [Masson-Delmotte. Cambridge University Press, Cambridge, United Kingdom and New York, NY, USA, pp 1513–1766. https://doi.org/10.1017/9781009157896.013

Silveira MVF, Silva-Junior CHL, Anderson LO, Aragão LEOC (2022) Amazon fires in the 21st century: the year of 2020 in evidence. Glob Ecol Biogeogr 31:2026–2040. https://doi.org/10.1111/geb.13577

Silvério DV, Oliveira RS, Flores BM (2022) Intensification of fire regimes and forest loss in the território indígena do Xingu. Environ Res Lett 17:045012. https://doi.org/10.1088/1748-9326/ac5713

Valencia S, Salazar JF, Hoyos N et al (2024) Current Forest–Savanna transition in Northern South America departs from typical Climatic thresholds. Ecosystems 27:61–76. https://doi.org/10.1007/s10021-023-00872-y

Vicente-Serrano SM, Beguería S, López-Moreno JI (2010) A multiscalar drought index sensitive to global warming: the standardized precipitation evapotranspiration index. J Clim 23(7):1696–1718. https://doi.org/10.1175/2009JCLI2909.1

Xu R, Yu P, Abramson MJ et al (2020) Wildfires, global climate change, and human health. N Engl J Med 383:2173–2181. https://doi.org/10.1056/NEJMsr2028985

Yang X, Zhao C, Zhao W, Fan H, Yang Y (2023) Characterization of global fire activity and its Spatiotemporal patterns for different land cover types from 2001 to 2020. Environ Res 227:115746. https://doi.org/10.1016/j.envres.2023.115746

Ynouye-Francés M, Ramos-Rodríguez MP, Martínez-Becerra LW et al (2021) Causalidad de Los incendios forestales En Pinar Del Río, Cuba (1975–2018). Colomb for 24:24–38. https://doi.org/10.14483/2256201x.16881

Zscheischler J, Seneviratne SI (2017) Dependence of drivers affects risks associated with compound events. Sci Adv 3(6). https://doi.org/10.1126/sciadv.1700263

Zscheischler J, Martius O, Westra S et al (2020) A typology of compound weather and climate events. Nat Reviews Earth Envir 1(7):333–347. https://doi.org/10.1038/s43017-020-0060-z